PROCEEDINGS OF SCIENCE

Study of initial- and final-state effects through polarization observables

N. Zachariou*
School of Physics and Astronomy, University of Edinburgh, James Clerk Maxwell Building, Peter Guthrie Tait Road, Edinburgh EH9 3FD,UK
E-mail: nick.zachariou@ed.ac.uk

D.P. Watts
School of Physics and Astronomy, University of Edinburgh, James Clerk Maxwell Building, Peter Guthrie Tait Road, Edinburgh EH9 3FD,UK

Y. Ilieva
School of Physics and Astronomy, University of South Carolina, Jones PSC, Columbia, SC 29208, USA

for the CLAS collaboration

The CEBAF Large Acceptance Spectrometer (CLAS) housed in Hall B of the Thomas Jefferson National Accelerator Facility (JLab) provides us with the experimental tools to study strongly-interacting matter and its dynamics. Polarization observables, accessible by means of polarised beams, allow us to perform detailed studies of the underlying dynamics of both initial- and final-state interactions as well as disentangle signal from background events. We have implemented this novel approach to study the interaction between hyperons and nucleons through final-state interactions in $\gamma d \to K^+ \Lambda n$, as well as study initial-state effects by direct comparison of reactions on bound (deuteron) and free-proton targets.

XVII International Conference on Hadron Spectroscopy and Structure - Hadron2017
25-29 September, 2017
University of Salamanca, Salamanca, Spain

*Speaker.

PoS(Hadron2017)147

1. Introduction

Detailed measurements of exclusive reactions on bound nucleons including polarization degrees of freedom provide us with crucial information to understand both initial- and final-state effects. Understanding initial-state effects are important to achieve a reliable determination of nucleon reactions in bound nucleon targets, an unavoidable complication for measuring reactions off the neutron. This is of particular current importance due to the need for accurate measurement of exclusive meson photoroduction off the neutron in the hunt for "missing" nucleon resonances, as some resonances are predicted to couple strongly to the neutron. Since no free-neutron targets exist, deuteron targets are typically employed, with the undesirable outcome that the determined observables are modified by both initial- and final-state effects. Here we investigate an approach to determine initial and final-state effects using polarization observables in a relatively model-independent way. Final-state effects would provide us with information on reactions involving short-lived particles that are otherwise experimentally challenging to perform. Specifically, constraining the hyperon-nucleon (YN) interaction would provide us with the missing ingredients to obtain a comprehensive and complete understanding of the strong-interaction including the strangeness degree of freedom. High-precision data from pure YN scattering experiments remain elusive due to the short hyperon lifetime. Because of this, information on the YN interaction has been typically inferred from hyper-nuclear studies in a model-dependent way. Final-state interactions (FSI) in exclusive hyperon photoproduction provide us with a complementary approach to study the YN interaction; one that is largely free from medium-modification and many-body effects. Here, we discuss our work on studying the YN interaction through FSI in the reaction $\gamma d \to K^+\Lambda n$. The studies presented here were performed using data obtained at JLab with CLAS [1] in experiment E06-103 [2].

2. Experimental setup

The Continuous Electron Beam Accelerator Facility (CEBAF) at JLab provided the polarized electron beam for the experiment with energies up to 6 GeV and electron polarizations $> 80\%$ [3]. The beam was delivered simultaneously to three experimental end stations (Halls A, B, and C) for complimentary research programs. The CLAS detector was the main scientific instrument for experiments performed in Hall B and provided a nearly 4π angular acceptance for charged-particler eaction products. The 6-GeV program of JLab was completed in 2012 and detector systems in all three end stations and accelerator have now been upgraded to receive and deliver electron beams up to 12 GeV[4]. The CLAS detector was comprised of three layers of drift chambers to measure charged-particle trajectories as they traversed the ϕ-direction magnetic field produced by six kidney-shaped superconducting coils, scintillators to measure time of flight, Čerenkov counters to separate electron from π^-, and electromagnetic calorimeters used primarily for photon and neutron identification (see left panel of Fig. 1). The CLAS detector provided an efficient detection of charged particles between 8° and 144° polar angles, with momentum and angular resolution of $\sim 0.5\%$ and 2 mrad, respectively.

Real-photon experiments were performed using the Hall-B Tagger spectrometer placed upstream of CLAS (see right panel of Fig. 1). Photons with energies between 20% and 95% of the

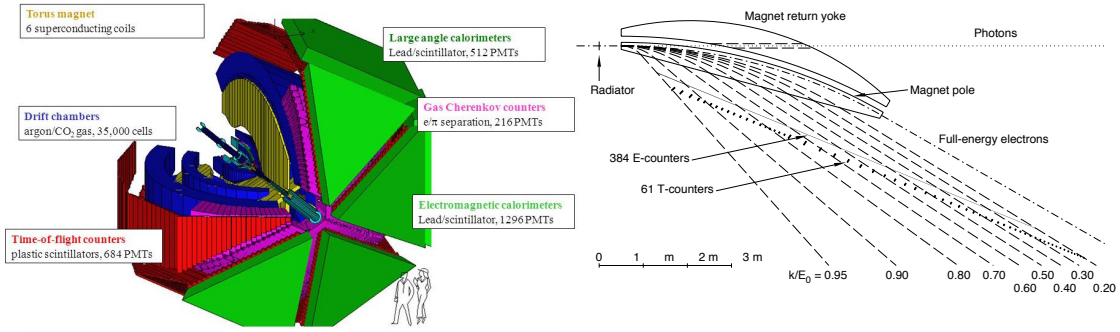

Figure 1: Left: A schematic of the CLAS detector. The kidney-shaped superconducting coils are shown in yellow, drift chambers in blue, Čerenkov counters in magenta, time-of-flight scintillators in red, and electromagnetic calorimeters in green. Right: The Hall-B photon tagging system located upstream of the CLAS detector.

incident electron energy E_0 were tagged with energy and timing resolution of $0.001E_0$ and 110 ps, respectively. Both circularly- and linearly-polarized photons beams were produced with the use of amorphous and crystal radiators. The degree of polarization of the linearly-polarized photon beam was on average 75% and that of the circularly-polarized photon beams was reaching 80% as $E_\gamma/E_0 \to 1.0$. These capabilities allowed the precise determination of a large set of polarization observables in exclusive reactions, providing the experimental tools needed to study initial- and final-state effects.

3. YN interaction through FSI

Our current knowledge of the strong force stems from the plethora of high-precision scattering experiments between nucleons. The investigation of the YN interaction, which is currently poorly constrained, is crucial in obtaining a comprehensive picture of the strong interaction. In addition, reliable and precise data on the interaction between hyperons and nucleons will allows us to address the “Hyperon Puzzle" [5], which reflects how theoretical models cannot predict the role of hyperons in neutron stars in a manner that is consistent with the most recent observations of massive neutron stars. As mentioned before, scattering experiments involving hyperons constitute a daunting task for experimentalists due to the short lifetime of hyperons. Final-state interactions in exclusive hyperon photoproduction reactions allow us to obtain a clear insight in the dynamics of the YN interaction and place very stringent constraints on existing theoretical models. Polarization observables are particularly important as they provide us with the constraints needed to identify and separate signal from background reactions in a (relatively) model-independent way.

The reaction $\gamma d \to K^+\Lambda n$ was reconstructed by identifying the final-state kaon as well as the proton and negative pion from the Λ-hyperon decay and selecting events in which the missing-mass, M_X, of $\gamma d \to K^+\Lambda X$ corresponded to the mass of the neutron (see left panel of Fig, 2). The momentum of the missing nucleon was also reconstructed, and the FSI sample was identified by selecting events in which the neutron momentum was higher than the typical Fermi momentum (p_X >200 MeV/c). The right panel of Fig. 2 shows the momentum of the missing neutron (blue points) compared with simulations that include the momentum distribution of a bound nucleon

(green points) calculated from the Paris potential, as well as the momentum distribution of events in which the nucleon is part of FSI (black line). The FSI contributions result from three main mechanisms as depicted in Fig. 3: the pion mediated reaction (panel b), the kaon-neutron rescattering (panel c), and the hyperon-nucleon rescattering (panel d). The data sample with missing momenta, $p_X < 150$ MeV/c is dominated by the quasi-free reaction (depicted in panel a).

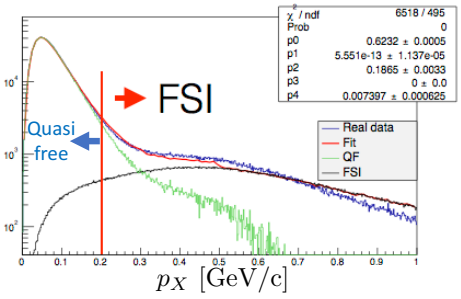

Figure 2: Missing momentum in the reaction $\gamma d \to K^+\Lambda X$ indicating the cut applied to select FSI. Simulated data for the quasi-free reaction (green) and the three FSI mechanisms shown in Fig. 3 (black) were fitted to experimental data (blue) to establish the relative contributions of the various mechanisms.

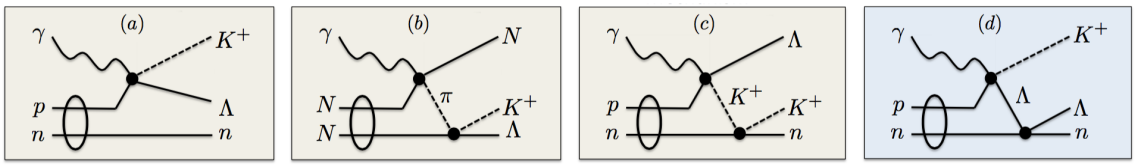

Figure 3: Four main mechanisms that contribute to the reaction $\gamma d \to K^+\Lambda n$ according to theoretical models [6, 7]: (a) quasi-free Λ photoproduction on the proton; (b) pion mediated production; (c) K^+ rescattering off the spectator neutron; (d) Λ rescattering offthe spectator neutron.

The linearly- and circularly- polarized photon beams produced with the Tagger facility in Hall B and the self-analyzing nature of the Λ hyperon, allow the simultaneous determination of a large set of polarization observables. Equation (3.1) shows the polarization observables accessible in our experiment

$$\frac{d\sigma}{d\Omega} = \left(\frac{d\sigma}{d\Omega}\right)_0 [1 - P_{lin}\Sigma\cos 2\phi + \alpha\cos\theta_x(-P_{lin}O_x\sin 2\phi - P_{circ}C_x) \\ -\alpha\cos\theta_y(-P_y + P_{lin}T\cos 2\phi) - \alpha\cos\theta_z(P_{lin}O_z\sin 2\phi + P_{circ}C_z)\ldots], \quad (3.1)$$

where $\left(\frac{d\sigma}{d\Omega}\right)_0$ is the unpolarized cross section, P_{lin} and P_{circ} are the degree of linear and circular polarizations, respectively, and Σ, O_x, O_z, , C_x, C_z, P_y, and T are the polarization observables. The azimuthal angle of the kaon, ϕ, is measured from the photon-polarization plane, and the direction cosines of the decay proton, $\cos\theta_{x,y,z}$, are measured in the Λ rest frame with the z axis given by the photon direction and the y axis by the photon-kaon plane (see Fig 4). The self-analyzing power of Λ, which allows the determination of the Λ polarization by studying the angular distribution of its decay products, is denoted by α.

The beam-spin asymmetry Σ can be obtained independently of the double-polarization observables using any of the final state particles (K^+, Λ, or n). This provides us with an excellent tool to identify kinematic regimes where YN FSI dominate. Specifically, in a quasi-free sample the beam-spin asymmetry determined using the kaon azimuthal distribution, Σ_{K^+}, is consistent with the beam-spin asymmetry determined using the Λ azimuthal distribution, Σ_Λ, as the two particles go

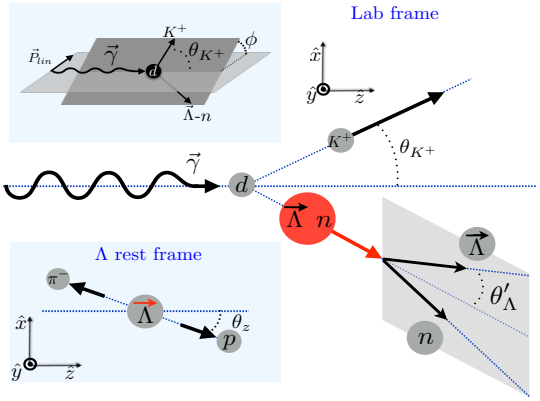

Figure 4: Reaction plane definition for $\gamma d \to K^+\Lambda n$. The upper left panel shows the definition of the kaon azimuthal angle ϕ with which Σ produces a modulation (see Eq. (3.1)). The lower left panel shows the definition of θ_z (and correspondingly θ_x) with which the double-polarization observables produce modulations. The main figure defines the kaon laboratory polar angle θ_{K^+}, and the hyperon angle $\theta_{\Lambda'}$, which is with respect to an axis pointing along the momentum of the YN pair.

back-to-back in their center-of-momentum frame. However, different FSI mechanisms dilute the magnitude of Σ in a predicted manner. For example, a kinematic regime where the pion-mediated reaction dominates, both beam-spin asymmetries, Σ_{K^+} and Σ_Λ, should vanish, but in a sample where the kaon-rescattering mechanism dominates, Σ_{K^+} is diluted but Σ_Λ is left unchanged. Similarly, in a YN-rescattering-dominated sample, Σ_Λ is diluted while Σ_{K^+} is left unchanged. Figure 5 shows the preliminary results from CLAS for Σ_{K^+} and Σ_Λ as a function of photon energy for an FSI dominated sample (left panel) and a quasi-free dominated sample (right panel). The determination

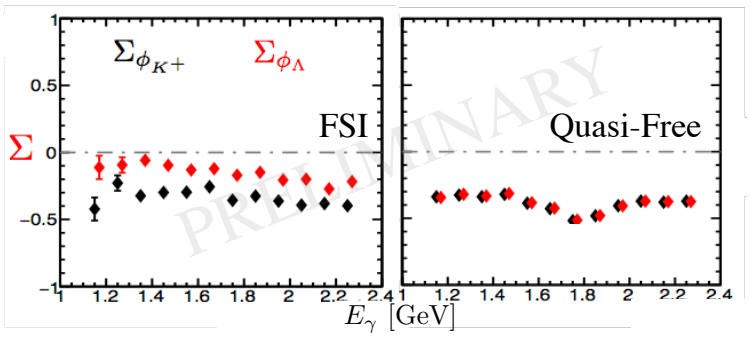

Figure 5: Beam-spin asymmetry Σ determined using the kaon (black points) and the hyperon (red points) azimuthal distribution for an FSI dominated sample (left panel) and a quasi-free dominate sample (right panel).

of all accessible polarization observables in kinematic regimes where YN FSI dominate allows us to place very stringent constraints on the underlying dynamics of the YN interaction and tune the existing and largely unconstrained YN potentials [6, 8]. The large CLAS data set allows us to obtain this set of observables and study their kinematical dependence, not only for one-fold differential kinematics, but also for up to three-fold differential kinematics, providing an unprecedented insight on the bare YN interaction.

4. Initial-state effects

It has been predicted that some nucleon resonances couple strongly to the neutron and therefore, for a detailed study of the excited nucleon spectrum, neutron targets need to be employed. Since no free neutron targets exist, bound neutron targets, the simplest of which is deuterium, are typically employed. The method discussed above allows us to establish contributions and the effects of FSI. In exclusive reactions initial-state effects can be significantly reduced or eliminated by studying the dependence of the observables on the momentum of the target nucleon. This approach

was investigated using reactions off the bound proton that allow us to directly compare the determined observables with ones that are determined using free-proton targets. Specificaly, the reaction $\gamma d \to K^+\Lambda n$ was used to determine a set of polarization observables and study their dependence on the missing momentum, p_X. The left panel of Fig. 6 shows the evolution of the beam-spin asymmetry for the quasi-free reaction. The horizontal line shows the determined observable when data with $p_X < 150$ MeV/c are used, an approach typically employed. The red dotted curve shows the approach employed in this analysis in which the observable of interest is determined with a polynomial extrapolation to $p_X \to 0$ MeV/c. The right panel of Fig. 6 compares the results extracted using the extrapolation method with recently published results obtained from free proton target. Our studies show that the determination of polarization observables utilizing a method that neglects the target nucleon momentum leads to estimates that are biased compared to ones that are determined by extrapolation to the free-nucleon point of $p_X = 0$ MeV/c.

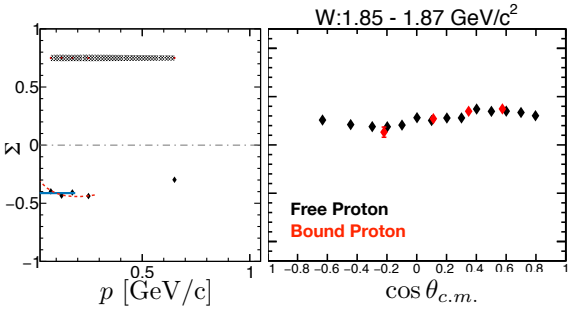

Figure 6: Evolution of Σ with target proton momentum determined using exclusive kaon photoproduction off the bound proton (left panel) and a comparison of results obtained through extrapolation with results off a free proton target. The blue solid line indicates the average value of the observable with $p_X < 200$ MeV/c and the dotted red line shows the fit to determine the extrapolated result.

References

[1] Mecking B. A. et. al. The CEBAF large acceptance spectrometer (CLAS). *Nucl. Instr. Meth.* A **503** 513-53 (2003).

[2] Nadel-Turonski P. N. et. al., Kaon production on the deuteron using polarized photons. Jefferson Lab Experiment E06-103 (2006).

[3] Leemann C. W., Douglas D R and Krafft G A, The Continuous Electron Beam Accelerator Facility: CEBAF at the Jefferson Laboratory, *Annu. Rev. Nucl. Part. Sci.* **51** 413-50 (2001).

[4] Burkert V. D., CLAS12 and its initial Science Program at the Jefferson Lab Upgrade. arXiv:0810.4718 (2008).

[5] Lonardoni D, Lovato A, Gandolfi S and Pederiva F, Hyperon Puzzle: Hints from quantum monte carlo calculations. *Phys. Rev. Lett.* **114** 092301-5 (2015).

[6] Salam A. et al., K^0photoproduction on the deuteron and the extraction of the elementary amplitude. *Phys. Rev. C* **74** 044004-8 (2006).

[7] Laget J. M., Pentaquark, cusp, and rescattering in single kaon photoproduction off deuterium. *Phys. Rev. C* **75** 014002-7 (2007).

[8] Miyagawa K. et al., Polarization observables in exclusive kaon photoproduction on the deuteron. *Phys. Rev. C* **74** 034002-11 (2006).